Warm photoionized plasmas created by soft-x-ray laser irradiation of solid targets

Mark Berrill,[1,*] Fernando Brizuela,[1] Benjamin Langdon,[1] Herman Bravo,[1] Carmen S. Menoni,[1] and Jorge J. Rocca[1,2]

[1]*NSF ERC for Extreme Ultraviolet Science and Technology and Department of Electrical and Computer Engineering, Colorado State University, Fort Collins, Colorado 80523, USA*

[2]*Department of Physics, Colorado State University, Fort Collins, Colorado 80523, USA*

[*]*Corresponding author: berrill@engr.colostate.edu*

Received January 8, 2008; revised February 9, 2008; accepted February 18, 2008; posted February 25, 2008 (Doc. ID 91422); published April 7, 2008

We report the study of warm plasmas created by soft-x-ray laser irradiation of solid targets in which single-photon photoionization is the dominant energy absorption mechanism. Low-absorption (silicon, $Z=14$) and high-absorption (chromium, $Z=24$, and silver, $Z=47$) targets were heated by ~1 ns duration pulses from a 46.9 nm wavelength soft-x-ray laser. The spectra obtained agree with 1 1/2-dimension simulations in showing that the Si plasmas are significantly colder and less ionized, confirming that in contrast to plasmas created by optical lasers the plasma properties are largely determined by the absorption coefficient of the target material.

OCIS codes: 140.7240, 350.5400, 300.2140.

1. INTRODUCTION

There is significant interest in the generation of plasmas with intense soft-x-ray laser beams [1,2]. The fundamentally different mechanisms by which intense soft-x-ray light interacts with materials defines a regime of laser–plasma interaction that differs significantly from that corresponding to plasmas created by optical lasers. The fact that soft-x-ray wavelengths are associated with critical densities that exceed solid density (e.g., $n_c=5\times10^{23}$ cm^{-3} for $\lambda=46.9$ nm light) results in greatly decreased Bremsstralung absorption and in the direct deposition of a large fraction of the laser pulse energy in the solid target, in which the initial depth of the heated region is determined mainly by the absorption coefficient of the material. The high photon energy of soft-x-ray beams exceeds the ionization energy of all neutral atoms and low-charge ions present, resulting in direct single-photon ionization of the plasma, an absorption mechanism unavailable to optical lasers. These fundamental disparities result in different energy deposition mechanisms and consequently in different plasma characteristics and dynamics. By using short soft-x-ray laser pulses, plasmas with very uniform conditions can be created over relatively large volumes [1].

The availability of high-intensity soft-x-ray lasers creates the opportunity to study the unique properties of plasmas created by intense monochromatic soft-x-ray light. Moreover, since soft-x-ray laser beams can be focused into spots less than 100 nm in diameter [3], the study of plasmas created by focused soft-x-ray lasers is of practical interest for the development of a new generation of nanoscale probes with analytic capabilities. Tabletop soft-x-ray laser beams generated by collisional electron impact excitation of ions in discharge-created and laser-created plasmas can be focused to generate plasmas with pulses ranging from the nanosecond [4] to the picosecond [5–11] time scales. The advent of soft-x-ray free electron lasers [12] will allow the study of plasmas heated by extremely intense soft-x-ray pulses in the complementary femtosecond time scale. In anticipation to experiments, theoretical studies have been conducted that predict that the characteristics of plasmas created with intense monochromatic soft-x-ray light will depend strongly on the target material and differ significantly from those created with visible lasers [2]. However, to our knowledge no experimental results of the study of the characteristics of such plasmas have been reported. A few groups have investigated the ablation of materials with focused soft-x-ray laser beams [3,4,13–16], but the studies concentrated on the effects on the ablated targets and not on the plasma phenomena.

Herein we report the spectroscopic study of plasmas created by focused soft-x-ray laser pulses of ~1 ns duration on solid targets and compare the results with hydrodynamic–atomic physics model simulations. Low-temperature plasmas were generated by irradiating low-Z (Si), and mid-Z (Cr and Ag) slab targets with the focused beam from a 46.9 nm wavelength (26.5 eV) Ne-like Ar capillary discharge soft-x-ray laser. The measurements show, in accordance with hydrodynamic model calculations, that the much lower absorption coefficient for Si at this wavelength results in plasmas that are significantly colder and less ionized than Cr and Ag plasmas, in spite of the faster expansion of the Cr and Ag plasmas. The nanosecond regime of soft-x-ray laser pulses investigated here differs and is complementary to the studies that will be conducted at soft-x-ray free electron lasers, which will employ pulses in the femtosecond time scale. In the nanosecond regime thermal heat conduction and expansion of

the plasma into vacuum play a significant role. Thermal conduction can increase the amount of ablated material, and expansion causes significant hydrodynamic cooling.

2. EXPERIMENTAL SETUP

A schematic diagram of the experimental setup is shown in Fig. 1. Si, Cr, and Ag targets were irradiated by the beam of a 46.9 nm Ne-like Ar capillary discharge soft-x-ray laser focused with a 10 cm radius of curvature spherical mirror. The laser pulses are produced by collisional electron impact excitation of Ne-like ions in a plasma column generated by a fast capillary discharge [17,18]. The plasma column is generated by injecting a 24 kA peak amplitude current pulse through a 3.2 mm diameter alumina capillary tube filled with ~410 mTorr of Ar gas. The current pulse rapidly compresses the plasma on axis, creating a hot and dense plasma in which Ne-like ions are excited to produce population inversion and gain in the $3p\ ^1S_0-3s\ ^1P_1$ line at 46.9 nm. In the configuration used in this experiment the laser produces pulses of ~100 μJ energy and 1.2 ns duration. The experiments were conducted in a vacuum chamber placed at 130 cm from the output of the laser. The laser beam was focused onto the target by using a mirror coated with Sc/Si multilayers [19], producing a focal spot of 10–15 μm diameter. The targets consisted of thin slabs that intersect part of the incoming laser beam (Fig. 1), reducing the irradiation fluence on target and making the focal spot slightly asymmetric. Shots with reduced irradiation energy were obtained by attenuating the beam with 0.2 μm thick, freestanding Al foils with measured transmissivity of ~17% at 46.9 nm. The targets were placed on a motorized translation stage that allowed the selection of the irradiated area and distance to the focusing mirror.

Light emitted by the plasma was collected by a 10 cm focal length fused silica lens to create a 1-to-1 image of the plasma onto the entrance slit of a 0.3 m focal length visible–ultraviolet spectrometer. The dispersed light was detected by using a back-illuminated CCD detector array. The light collection system was sufficiently efficient to produce line spectra from a single laser shot. However, most spectra were obtained by accumulating several laser shots to improve the signal-to-noise ratio.

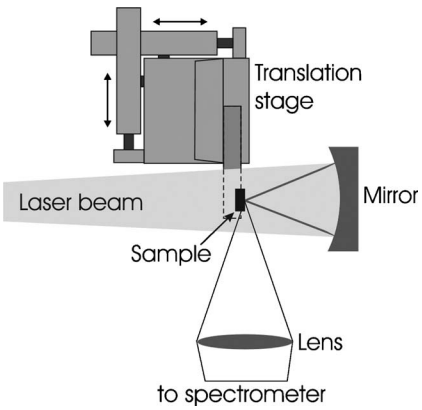

Fig. 1. Experimental setup used for the generation and spectroscopy of soft-x-ray laser-created plasma. The vacuum chamber is not shown.

Similar experiments were performed by irradiating the samples with 120 ps optical laser pulses ($\lambda = 800$ nm) produced by a Ti:sapphire laser system consisting of a mode-locked oscillator, a grating stretcher, and a multipass amplifier. In this case the laser beam was focused into a ~35 μm diameter spot by a 15 cm focal length fused silica lens. Spectra of the resulting plasmas were recorded by using the same setup.

3. EXPERIMENT AND SIMULATION RESULTS

Experiments were conducted by irradiating the targets with three different soft-x-ray laser pulse energies, 0.5, 3.1, and 17 μJ, corresponding to peak intensities of 4×10^8, 2.5×10^9, and 1.4×10^{10} W/cm^2, respectively. The plasmas were modeled with a 1 1/2-dimension hydrodynamic-atomic code [20]. The hydrodynamic equations were solved in 1D, with the lateral expansion taken into account using the self-similar solution for expansion into a vacuum [21]. The 1 1/2-dimension code includes a collisional–radiative atomic model with multicell radiation transport, which solves for the ground state and excited populations by using a quasi-steady-state solution. Both inverse Bremsstrahlung absorption as well as photoionization are included as energy deposition mechanisms for the soft-x-ray laser. Photoionization absorption is calculated by using the ion distribution from the atomic model, with the photoionization cross section for each ion. The atomic data is obtained from the Flexible Atomic Code (FAC) [22] with photoionization cross sections from Reilman and Manson [23]. A postprocessor was used to synthesize spectra based on multicell radiation transport and the computed populations and opacities. To improve the accuracy of the synthesized spectra the level energies and transition probabilities were calibrated by using experimental data when available [24].

At the lowest irradiation energy investigated, 0.5 μJ, all three elements were found to be below the ablation threshold, in agreement with the simulations. At the intermediate energy of 3.1 μJ plasma radiation from neutral Cr and Ag atoms was observed [Figs. 2(c) and 2(e)]. At this energy Si is very close to the ablation threshold, resulting in only very weak emission from two of the strongest Si I lines in the ultraviolet spectra [Fig. 2(a)]. These observations agree with model simulations that predict that the Cr and Ag plasmas reach a peak temperature of 2.2 and 2.8 eV and a peak degree of ionization of $Z = 0.5$ and $Z = 1.0$, respectively while Si, which is at the threshold of ablation, only reaches a peak temperature of 0.2 eV and a degree of ionization $Z < 0.01$. The different behavior of these materials is to be expected, as the absorption length of the 46.9 nm laser light in Si (~300 nm) greatly exceeds that of Cr and Ag (~18 and ~7.5 nm, respectively) Consequently, in Si the soft-x-ray light interacts with a much larger volume of material, which results in a higher ablation threshold and in a colder plasma.

At the highest irradiation energy (17 μJ) plasma radiation was observed for all three elements. Figure 2 shows the measured time-integrated visible spectra corresponding to Si [Fig. 2(b)], Cr [Fig. 2(d)], and Ag [Fig. 2(f)] plasmas for this irradiation condition. The Si spectrum of Fig.

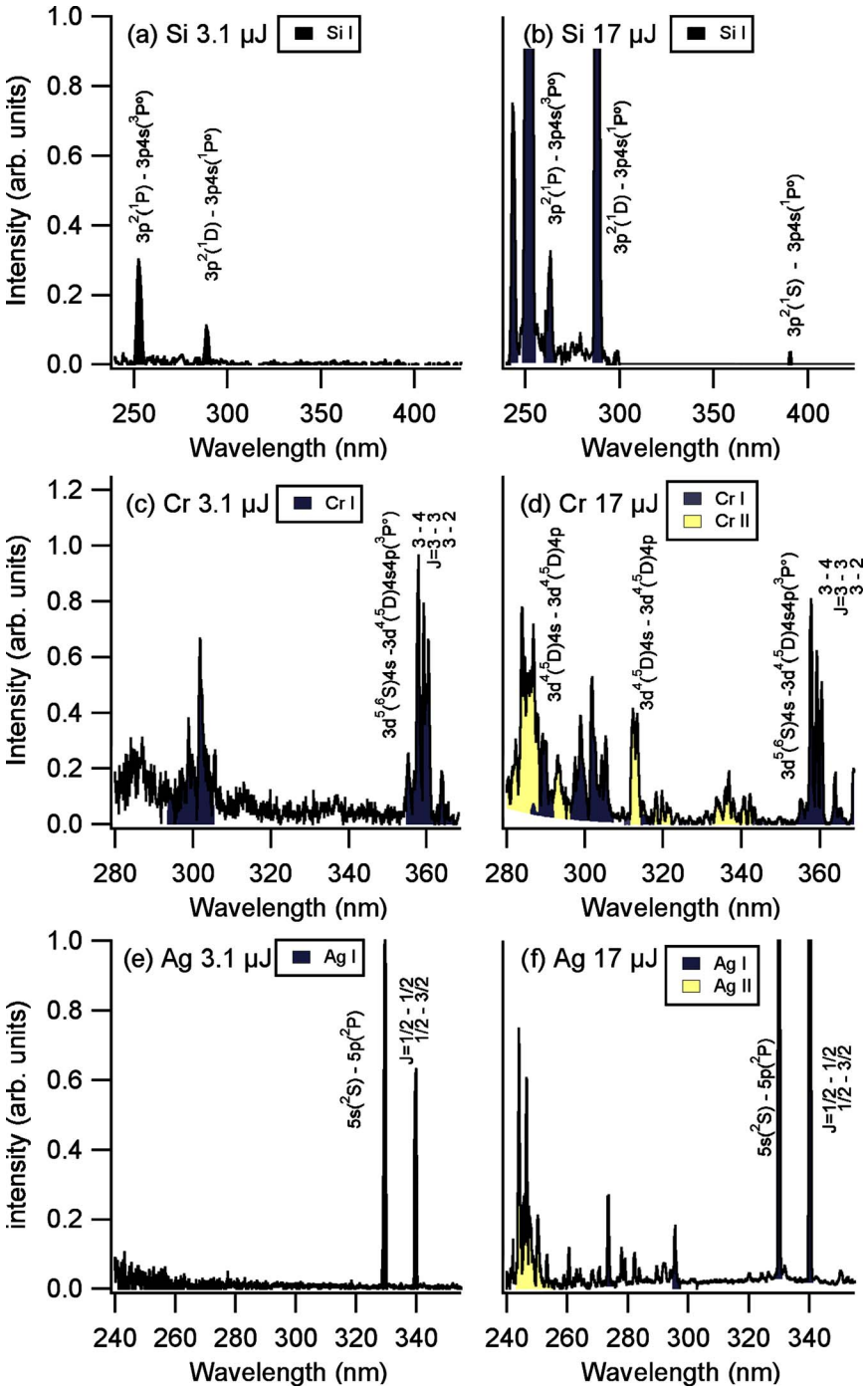

Fig. 2. (Color online) Spectra of Si, Cr, and Ag plasmas created by irradiating solid targets with 3.1 and 17 μJ, 46.9 nm soft-x-ray laser pulses. At 3.1 μJ (a) Si is only slightly above the ablation threshold, while for both (c) Cr and (e) Ag strong lines from the neutral atoms are present. At 17 μJ only neutral atom lines are present for (b) Si, while the (d) Cr and (f) Ag spectra show lines from both the neutral atoms and the singly charged ions.

2(b) still displays only lines associated with neutral Si (Si *I*). Classified lines from singly charged silicon (Si II) that fall within the spectral window of the measurement (e.g., 207.27, 290.43, and 290.57 nm) are not observed, an indication that this is a very low-temperature plasma, in agreement with model calculations. In contrast, spectra of plasmas created by irradiation of Cr and Ag targets with the same soft-x-ray laser intensity show lines of Cr II and Ag II [Figs. 2(d) and 2(f)]. Figure 3 shows the computed plasma parameters for Si and Cr plasmas created under these irradiation conditions. The peak temperature for Si is 1.1 eV [Fig. 3(a)], while Cr reaches a significantly higher temperature of 4.5 eV [Fig. 3(b)]. This again reflects the difference in the photoionization cross sections at 46.9 nm: 6.1×10^{-19} cm^2 and 9.5×10^{-18} cm^2 for Si and Cr, respectively. This difference in the cross-section results in more energy being absorbed by fewer atoms for Cr than for Si. The larger Cr plasma temperature results in a computed peak degree of ionization of 1.6 for Cr as compared with a degree of ionization of only 0.25 for Si

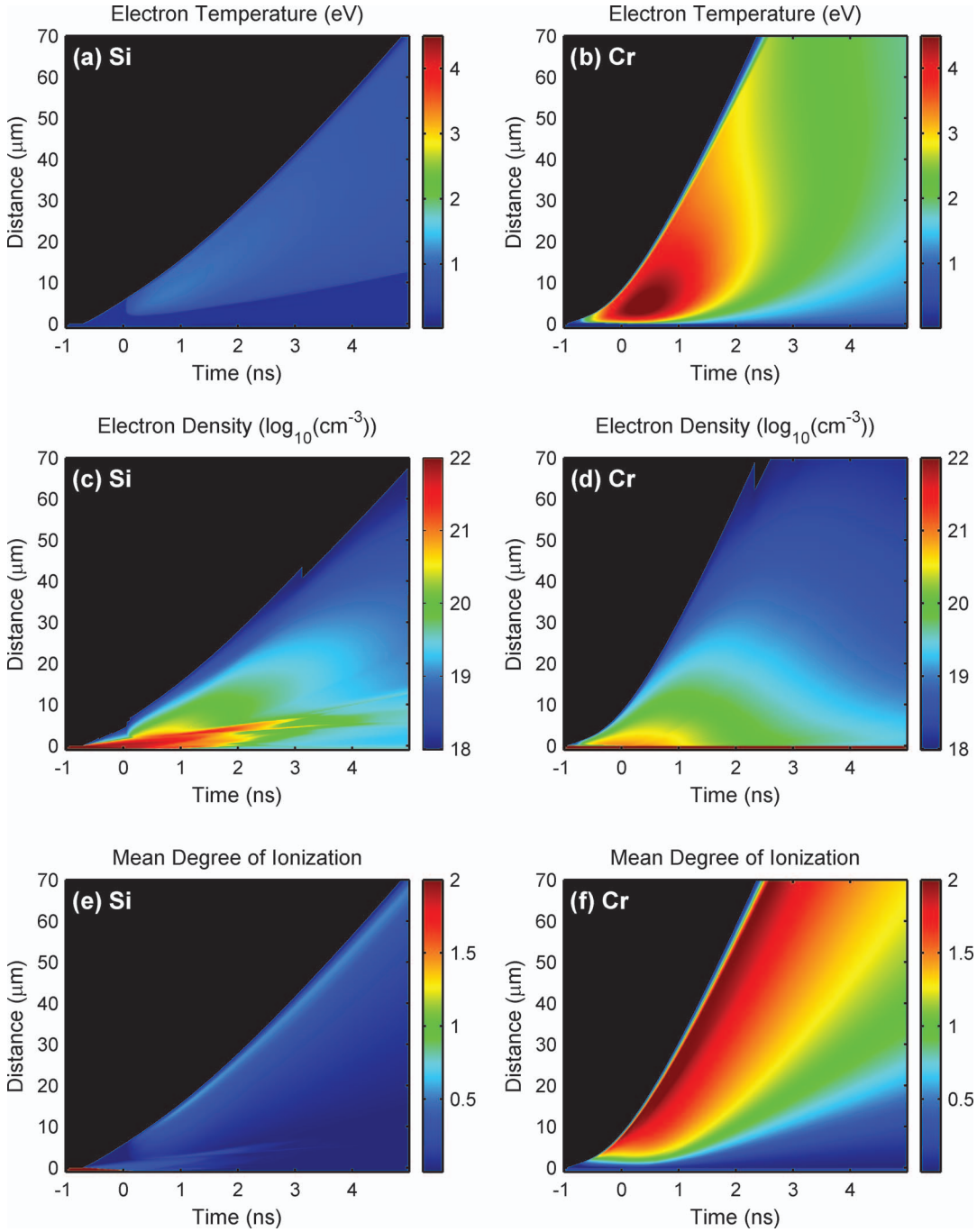

Fig. 3. Computed plasma parameters corresponding to Si and Cr plasmas generated by 17 μJ energy, 1.2 ns duration soft-x-ray laser pulse irradiation ($\lambda = 46.9$ nm) of solid targets. Because of the smaller absorption cross section (a) the Si plasma is significantly colder than (b) the Cr plasma. (d) The Cr plasma expands at a significantly higher rate. Due to the lower temperature (e) the Si plasma has a much lower degree of ionization than (f) the Cr plasma.

[Figs. 3(f) and 3(e), respectively]. Owing to the higher temperature, the Cr plasma has an increased expansion velocity [Figs. 3(c) and 3(d)], which results in significantly denser plasma away from the target surface.

Figure 4 shows simulated spectra for Si and Cr for the irradiation conditions corresponding to the experimental spectra of Figs. 2(b) and 2(d). The computed Si spectra resembles well that observed in the experiments, showing only Si I lines. The synthesized Cr spectrum also reproduces most of the features of the experimental data, but shows a slightly larger ratio between Cr II and Cr I lines and the presence of weak Cr III lines. This is in part because the synthetic spectra is calculated for the plasma conditions on axis of the irradiated spot, where the plasma has the highest temperature. A 2D plasma model would be necessary to further improve the agreement between the computed and the measured spectra. However, some of the differences are due to an incomplete assignment of the energy levels, while others can arise from the bundling of lines in the calculations. The latter is required for computation efficiency, because there are ~1350 levels of interest in the neutral and first ion of Cr,

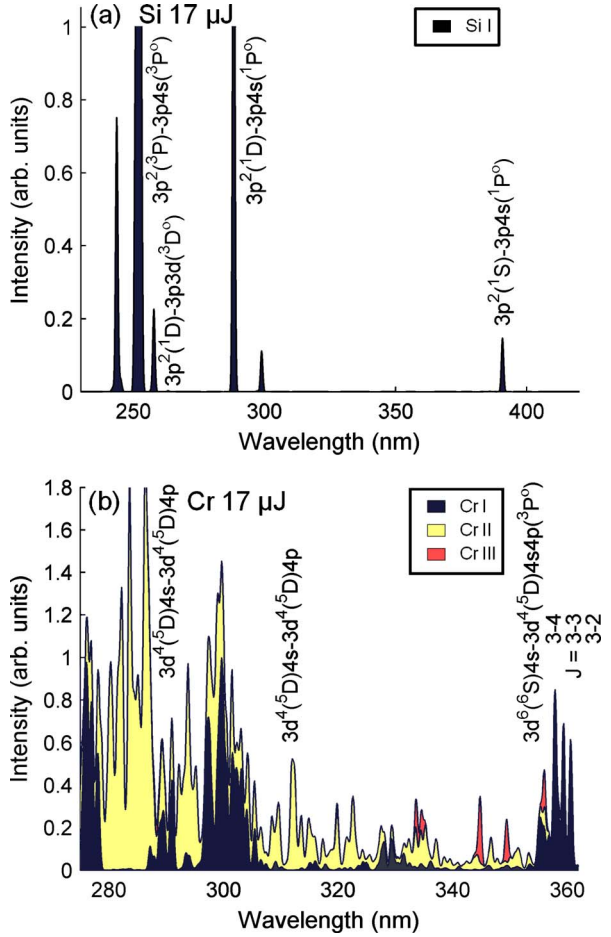

Fig. 4. (Color online) Simulated spectra for Si and Cr plasmas created by 17 μJ soft-x-ray laser ($\lambda = 46.9$ nm) pulse irradiation. (a) The Si spectrum is completely dominated by neutral atom lines (Si *I*) (a), while (b) the hotter Cr spectra contain large numbers of both Cr *I* and Cr II lines.

emitting over 100,000 lines. Nevertheless, the computed and measured spectra agree, clearly showing the signatures of a significantly less ionized, colder Si plasma.

This behavior of the soft-x-ray laser-created plasmas is in contrast to that of plasmas created by irradiation with visible wavelengths, which do not show such strong elemental dependence. In plasmas created with a visible-light laser, once the ablation threshold has been reached, most of the heating occurs via inverse Bremsstrahlung absorption in the plasma near the critical density (1.7×10^{21} cm^{-3} for 800 nm), which is independent of the elemental composition of the target. To verify this different behavior Ti:sapphire laser pulse energies of 97 μJ (a few times above the ablation threshold of $\sim$25 μJ) and 170 μJ were used to irradiate Si and Cr samples (Fig. 5). At 97 μJ, Si *I*, Si II, and weak Si III lines are observed in the silicon spectra, and Cr *I* and Cr II lines in the Cr spectra. For 170 μJ, strong Si *I*, Si II, and Si III lines are present, while the ratio of Cr II to Cr *I* lines increases slightly. The spectra indicate that the degree of ionization for both elements is similar, in sharp contrast to the case of irradiation with soft-x-ray light, where for all laser energies Si is observed to be less ionized than Cr because of the significant differences in the photoionization cross section. In addition to the elemental dependence the soft-x-ray laser plasmas can be expected to exhibit a strong wavelength dependence [2], governed by the relative position of the laser wavelength respect to the absorption edges of the material.

Simulations were also conducted for higher irradiation energies. The results show that as the intensity of the soft-x-ray laser is increased, the behavior of the different elements tends to converge. When the laser energy is increased by a factor of 10, the temperature of the Si plasma is computed to increase slightly above 3.5 eV, while that of the Cr and Ag plasmas increases to 9.0 and 6.5 eV respectively. Additionally, the mean degree of ionization increases to $Z = 1.4$ for Si and to 2.5 and 2.7 for both Cr and Ag. If the laser energy is further increased by a factor of 100, to 1.7 mJ, the electron temperature is computed to reach 7 eV for Si, 16 eV for Cr, and 10 eV for Ag, while the degree of ionization of the Si plasma, $Z = 2.5$, is calculated to approach that for Cr and Ag, $Z = 3.0$ and $Z = 3.2$. The predicted convergence of the plasma parameters as the irradiation flux is increased is caused by the fact that the amount of mass ablated from the three materials tends to equalize at increased irradiation. This is caused by the more rapid increase in the degree of ionization for Cr and Ag that causes these plasmas to become more rapidly transparent than Si to the 25 eV laser photons (depleted of the absorbing neutral and singly charged ions). At high irradiation energies plasmas with a very uniform degree of ionization can be created. For example, the degree of ionization of a Ag plasma created under the high-intensity condition (1 ns after the peak of a 1.7 mJ laser pulse) is computed to vary by less than 10% over 90% of the entire plasma volume. However, the plasma density within the volume changes significantly owing to expansion. The degree of ionization at which the plasma becomes transparent increases with decreasing laser wavelength. Therefore shorter-wavelength soft-x-ray lasers will create hotter plasmas and preserve the differences between elements until the plasma reaches a higher degree of ionization.

The behavior of the plasmas that will be generated by femtosecond soft-x-ray laser pulses will maintain the strong elemental dependence, but important differences exist. Because of the short pulse duration thermal conduction and expansion do not play a significant role. For the nanosecond-duration soft-x-ray laser pulses used in our experiment the ablation depth can be significantly deeper than the penetration of the soft-x-ray light owing to thermal conduction into the solid target during and after pulse irradiation. For example, at 17 μJ the ablation depth of Si is $\sim$1000 nm, corresponding to $\sim 3\times$ its absorption length (320 nm), while for Cr the ablation depth is $\sim$100 nm, which is $\sim 8\times$ the absorption length (13 nm). By contrast, for femtosecond pulses thermal conduction is insignificant during the pulse, yielding ablation depths that more closely match the absorption length. Additionally, expansion of the plasma during the laser pulse is dramatically reduced for a femtosecond pulse. As a result, the plasma density is much more uniform than for the 1 ns pulses studied. This will allow the generation of large plasma volumes with nearly constant temperature, density, and degree of ionization.

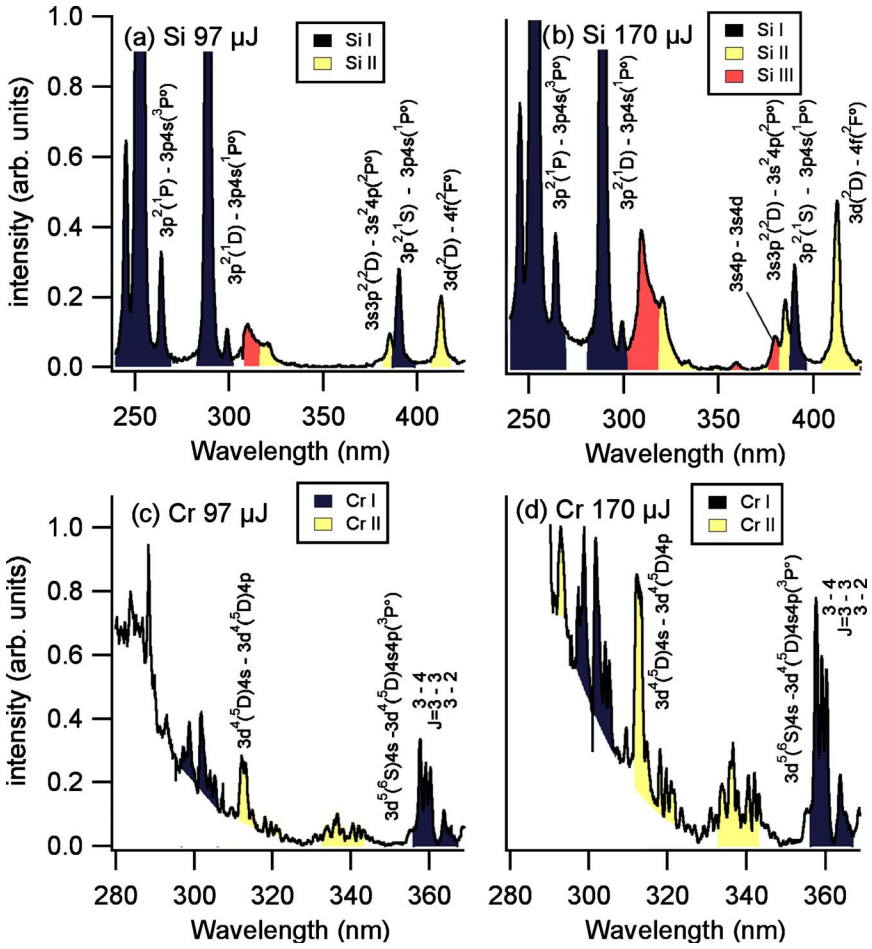

Fig. 5. (Color online) Spectra of (a), (b) Si and (c), (d) Cr created by $\lambda = 800$ nm laser pulses of 120 ps duration. Si II, Si III, and Cr II lines are emitted from the plasmas created by the 90 and 170 μJ pulses.

4. CONCLUSIONS

We have studied warm plasmas generated by focusing 46.9 nm soft-x-ray laser pulses of nanosecond duration onto Si, Cr, and Ag solid targets. The critical density corresponding to this wavelength (5×10^{23} cm^{-3}) exceeds the solid density, and absorption is dominated by single-photon photoionization. Spectra of the soft-x-ray laser-created plasmas were compared with those of plasmas created with an optical ($\lambda = 800$ nm) laser. The results agree with hydrodynamic model calculations in showing that the soft-x-ray laser plasmas differ from those created by visible lasers and are strongly element dependent, with characteristics largely determined by the position of the laser wavelength relative to absorption edges and resonances. Measured spectra agree with model simulations in showing that soft-x-ray laser-created Si plasmas, for a low-absorption material at 46.9 eV, are significantly colder and less ionized than plasmas created from more highly absorbent materials such as Cr and Ag. This strong elemental dependence is computed to soften at higher nanosecond pulse irradiation intensities that deplete the low-charge species, whose photoionization cross sections dominate the plasma absorption. High-intensity soft-x-ray lasers generating shorter pulses will be able to create highly uniform warm dense plasma over large volumes.

ACKNOWLEDGMENTS

This work supported by the National Nuclear Security Administration under the Stewardship Science Academic Alliances program through U.S. Department of Energy (DOE) Grant DE-FG52-06NA26152, using facilities from the National science Foundation (NSF) Engineering Research Center for Extreme Ultraviolet Science and Technology, NSF Award EEC-0310717. M. Berrill acknowledges support from the DOE Computational Science Graduate Fellowship under grant DE-FG02-97ER25308.

REFERENCES

1. R. W. Lee, S. J. Moon, H. K. Chung, W. Rozmus, H. A. Baldis, G. Gregori, R. C. Cauble, O. L. Landen, J. S. Wark, A. Ng, S. J. Rose, C. L. Lewis, D. Riley, J.-C. Gauthier, and P. Audebert, "Finite temperature dense matter studies on next-generation light sources," J. Opt. Soc. Am. B **20**, 770–778 (2003).
2. M. Fajardo, P. Zeitoun, and J.-C. Gauthier, "Hydrodynamic simulation of XUV laser-produced plasmas," Eur. Phys. J. D **29**, 69–75 (2004).
3. G. Vaschenko, A. Garcia Etxarri, C. S. Menoni, J. J. Rocca, O. Hemberg, S. Bloom, W. Chao, E. H. Anderson, D. T. Attwood, Y. Lu, and B. Parkinson, "Nanometer scale ablation with a table-top soft-x-ray laser," Opt. Lett. **31**, 3615–3617 (2006).
4. B. R. Benware, A. Ozols, J. J. Rocca, I. A. Artioukov, V. V.

Kondratenko, and A. V. Vinogradov, "Focusing of a tabletop soft-x-ray laser beam and laser ablation," Opt. Lett. **24**, 1714–1716 (1999).
5. J. Dunn, Y. Li, A. L. Osterheld, J. Nilsen, J. R. Hunter, and V. N. Shlyaptsev, "Gain saturation regime for laser-driven tabletop, transient Ni-like ion x-ray lasers," Phys. Rev. Lett. **84**, 4834–4837 (2000).
6. K. A. Janulewicz, A. Lucianetti, G. Priebe, W. Sandner, and P. V. Nickles, "Saturated Ni-like Ag x-ray laser at 13.9 nm pumped by a single picosecond laser pulse," Phys. Rev. A **68**, 051802 (2003).
7. Y. Wang, M. A. Larotonda, B. M. Luther, D. Alessi, M. Berrill, V. N. Shlyaptsev, and J. J. Rocca, "Demonstration of high-repetition-rate tabletop soft-x-ray lasers with saturated output at wavelengths down to 13.9 nm and gain down to 10.9 nm," Phys. Rev. A **72**, 053807 (2005).
8. M. A. Larotonda, Y. Wang, M. Berrill, B. M. Luther, J. J. Rocca, M. M. Shakya, S. Gilbertson, and Z. Chang, "Pulse duration measurements of grazing incidence pumped high repetition rate Ni-like Ag and Cd transient soft-x-ray lasers," Opt. Lett. **31**, 3043–3045 (2006).
9. Ph. Zeitoun, G. Faivre, S. Sebban, T. Mocek, A. Hallou, M. Fajardo, D. Aubert, Ph. Balcou, F. Burgy, D. Douillet, S. Kazamias, G. de Lachèze-Murel, T. Lefrou, S. le Pape, P. Mercère, H. Merdji, A. S. Morlens, J. P. Rousseau, and C. Valentin, "A high-intensity highly coherent soft x-ray femtosecond laser seeded by a high harmonic beam," Nature **431**, 426–429 (2004).
10. Y. Wang, E. Granados, M. A. Larotonda, M. Berrill, B. M. Luther, D. Patel, C. S. Menoni, and J. J. Rocca, "High-brightness injection-seeded soft-x-ray-laser amplifier using a solid target," Phys. Rev. A **22**, 123901 (2006).
11. Y. Wang, E. Granados, F. Pedaci, D. Alessi, B. Luther, M. Berrill, and J. J. Rocca, "Phase-coherent, injection-seeded, table-top soft-x-ray lasers at 18.9 nm and 13.9 nm," Nat. Photonics **2**, 94–98 (2008).
12. W. Ackermann, G. Asova, V. Ayvazyan, A. Azima, N. Baboi, J. Bähr, V. Balandin, B. Beutner, A. Brandt, A. Bolzmann, R. Brinkmann, O. I. Brovko, M. Castellano, P. Castro, L. Catani, E. Chiadroni, S. Choroba, A. Cianchi, J. T. Costello, D. Cubaynes, J. Dardis, W. Decking, H. Delsim-Hashemi, A. Delserieys, G. Di Pirro, M. Dohlus, S. Düsterer, A. Eckhardt, H. T. Edwards, B. Faatz, J. Feldhaus, K. Flöttmann, J. Frisch, L. Fröhlich, T. Garvey, U. Gensch, Ch. Gerth, M. Görler, N. Golubeva, H.-J. Grabosch, M. Grecki, O. Grimm, K. Hacker, U. Hahn, J. H. Han, K. Honkavaara, T. Hott, M. Hüning, Y. Ivanisenko, E. Jaeschke, W. Jalmuzna, T. Jezynski, R. Kammering, V. Katalev, K. Kavanagh, E. T. Kennedy, S. Khodyachykh, K. Klose, V. Kocharyan, M. Körfer, M. Kollewe, W. Koprek, S. Korepanov, D. Kostin, M. Krassilnikov, G. Kube, M. Kuhlmann, C. L. S. Lewis, L. Lilje, T. Limberg, D. Lipka, F. Löhl, H. Luna, M. Luong, M. Martins, M. Meyer, P. Michelato, V. Miltchev, W. D. Möller, L. Monaco, W. F. O. Müller, O. Napieralski, O. Napoly, P. Nicolosi, D. Nölle, T. Nuñez, A. Oppelt, C. Pagani, R. Paparella, N. Pchalek, J. Pedregosa-Gutierrez, B. Petersen, B. Petrosyan, G. Petrosyan, L. Petrosyan, J. Pflüger, E. Plönjes, L. Poletto, K. Pozniak, E. Prat, D. Proch, P. Pucyk, P. Radcliffe, H. Redlin, K. Rehlich, M. Richter, M. Roehrs, J. Roensch, R. Romaniuk, M. Ross, J. Rossbach, V. Rybnikov, M. Sachwitz, E. L. Saldin, W. Sandner, H. Schlarb, B. Schmidt, M. Schmitz, P. Schmüser, J. R. Schneider, E. A. Schneidmiller, S. Schnepp, S. Schreiber, M. Seidel, D. Sertore, A. V. Shabunov, C. Simon, S. Simrock, E. Sombrowski, A. A. Sorokin, P. Spanknebel, R. Spesyvtsev, L. Staykov, B. Steffen, F. Stephan, F. Stulle, H. Thom, K. Tiedtke, M. Tischer, S. Toleikis, R. Treusch, D. Trines, I. Tsakov, E. Vogel, T. Weiland, H. Weise, M. Wellhöfer, M. Wendt, I. Will, A. Winter, K. Wittenburg, W. Wurth, P. Yeates, M. V. Yurkov, I. Zagorodnov, and K. Zapfe, "Operation of a free-electron laser from the extreme ultraviolet to the water window," Nat. Photonics **1**, 336–342 (2007).
13. M. Grisham, G. Vaschenko, C. S. Menoni, J. J. Rocca, Yu. P. Pershyn, E. N. Zubarev, D. L. Voronov, V. A. Sevryukova, V. V. Kondratenko, A. V. Vinigradov, and I. A. Artioukov, "Damage to extreme-ultraviolet Sc/Si multilayer mirrors exposed to intense 46.9-nm laser pulses," Opt. Lett. **29**, 620–622 (2004).
14. L. Juha, M. Bittner, D. Chvostova, V. Letal, J. Krasa, Z. Otcenasek, M. Kozlova, J. Polan, A. R. Präg, B. Rus, M. Stupka, J. Krzywinski, A. Andrejczuk, J. B. Pelka, R. Sobierajski, L. Ryc, J. Feldhaus, F. P. Boody, M. E. Grisham, G. O. Vaschenko, C. S. Menoni, and J. J. Rocca, "XUV-laser induced ablation of PMMA with nano-, pico-, and femtosecond pulses," J. Electron Spectrosc. Relat. Phenom. **144**, 929–932 (2005).
15. M. Bittner, L. Juha, B. Rus, M. Kozlova, J. Krasa, Z. Otcenasek, J. Polan, A. R. Praeg, M. Stupka, L. Ryc, and R. H. Sobierajski, "Material ablation induced by focused 21.2-nm radiation from Ne-like Zn x-ray laser," Proc. SPIE **5777**, 965–969 (2005).
16. T. Mocek, B. Rus, M. Stupka, M. Kozlová, A. R. Präg, J. Polan, M. Bittner, R. Sobierajski, and L. Juha, "Focusing a multimillijoule soft x-ray laser at 21 nm," Appl. Phys. Lett. **89**, 051501 (2006).
17. J. J. Rocca, V. Shlyaptsev, F. G. Tomasel, O. D. Cortázar, D. Hartshorn, and J. L. A. Chilla, "Demonstration of a discharge pumped table-top soft-x-ray laser," Phys. Rev. Lett. **73**, 002192 (1994).
18. B. R. Benware, C. D. Macchietto, C. H. Moreno, and J. J. Rocca, "Demonstration of a high average power tabletop soft x-ray laser," Phys. Rev. Lett. **81**, 5804–5807 (1998).
19. Yu. A. Uspenskii, V. E. Lebashov, A. V. Vinogradov, A. I. Fedorenko, V. V. Kondratenko, Yu. P. Pershin, E. N. Zubalev, and V. Yu. Fedotov, "High-reflectivity multilayer mirrors for a vacuum-ultraviolet interval of 35–50 nm," Opt. Lett. **23**, 771–773 (1998).
20. M. A. Berrill, "A computer model to simulate laser created plasmas used for the generation of extreme ultraviolet light," M.S. thesis (Colorado State University, 2006).
21. G. J. Pert, "The hybrid model and its application for studying free expansion," J. Fluid Mech. **131**, 401–426 (1983).
22. M. F. Hu, "Indirect x-ray line-formation processes in iron *L*-shell ions," Astrophys. J. **582**, 1241–1250 (2003).
23. R. F. Reilman and S. T. Manson, "Photoabsorption cross sections for positive atomic ions with $Z \leq 30$," Astrophys. J., Suppl. Ser. **40**, 815–880 (1979).
24. NIST Atomic Spectra Database Version 3, http://physics.nist.gov/PhysRefData/ASD/index.html.